Electronic Supplementary Material (ESI)

Additive-associated antisolvent engineering of perovskite film for highly stable and efficient *p-i-n* perovskite solar cells

Rui Su,[a] Xudong Yang,[a] Wenxi Ji,[b] Taoyi Zhang,[b] Longgui Zhang, [b] Ailian Wang,[b] Zhixuan Jiang,[a] Qiaoyun Chen,[a] Yi Zhou*[a] and Bo Song*[a]

[a] *Laboratory of Advanced Optoelectronic Materials, Suzhou Key Laboratory of Novel Semiconductor-optoelectronics Materials and Devices, College of Chemistry, Chemical Engineering and Materials Science, Soochow University, Suzhou 215123, China Tel.: +86 (0) 512 65882507; E-mail: songbo@suda.edu.cn; yizhou@suda.edu.cn*

[b] *Sinopec (Beijing) Research Institute of Chemical Industry Co., Ltd, Beijing 100013, P.R. China*

Experimental section

Reagents and materials

Unless otherwise stated, all materials were purchased from Sigma–Aldrich or Alfa Aesar and used as received. Perovskite films and devices were fabricated using PbI_2 (99.999% purity) purchased from Alfa Aesar and taurine purchased from Shanghai Macklin Biochemical Co., Ltd. Formamidinium iodide (FAI), methylammonium bromide (MABr), lead bromide ($PbBr_2$), cesium iodide (CsI) (99.999% purity), poly(triarylamine) (PTAA), and bathocuproine (BCP; sublimed grade, 99.99% purity) were purchased from Xi'an Polymer Light Technology. C_{60} was purchased from Suzhou Dade Carbon Nanotechnology. ITO glass (<15 Ω/square) was purchased from Advanced Election Technology Co. Ltd. All anhydrous solvents were purchased from J&K Technology.

Devices Fabrication

The patterned ITO/glass substrates were sequentially cleaned with soap, deionized water, acetone, ethanol, and isopropanol twice each solvent and 15 min every time under ultrasonication. Before use, the ITO/glass substrates were dried in N_2 flow and treated with UV ozone for 15 min. The perovskite films were fabricated by the antisolvent crystallization approach in a glovebox filled with N_2. For the deposition of the HTLs, PTAA

was dissolved in toluene to obtain a 2 mg mL^{-1} solution, stirred overnight, spin-coated at 6000 rpm for 30 s in a glove box, and then annealed at 100 °C for 5 min. The perovskite precursor solution (1.4 M) composed of mixed cations (Pb, Cs, FA, and MA) and halides (I and Br) was dissolved in mixed solvents of dimethylformamide (DMF):dimethyl sulfoxide (DMSO) = 4:1 (volume ratio) according to the formula $Cs_{0.05}(FA_{0.92}MA_{0.08})_{0.95}Pb(I_{0.92}Br_{0.08})_3$. Afterward, the perovskite solution (60 μL) was spin-coated onto the ITO/PTAA substrate at 2000 rpm for 20 s and 4000 rpm for 40 s. Chlorobenzene (150 μL) was dropped on the spinning substrate during 30 s of the second spin-coating step. Subsequently, the sample was annealed at 70 °C for 5 min and then 100 °C for 10 min. To prepare the perovskite films treated with AAE, we added taurine in chlorobenzene and then undertook coating and heat treatment in the same way. Finally, C_{60} (20 nm)/BCP (8 nm)/Ag (80 nm) was deposited on the perovskite film by vacuum evaporation at 2×10^{-4} Pa. The device size area was 0.1 cm^2.

Characterization

Thermogravimetric analysis (TGA) measurements were performed on a Discovery TGA (Mettler Toledo Instruments, Switzerland) under dry nitrogen at 10 °C/min. XRD patterns were collected on a D2 PHASER diffractometer with Cu Kα radiation (Bruker, Germany). The *J–V* curves of the Pero-SCs were recorded using a Keithley 2400 source meter (Keithley Instruments, USA) in a glove box filled with N_2. The measurement was conducted under AM 1.5 G solar illumination with an intensity of 100 mW cm^{-2} in the reverse scan (RS) at a scan speed of 10 mV s^{-1}. The EQE curves were measured by using a solar cell spectral response measurement system QE-R3011 (Enli Technology Co., Ltd, Taiwan) in the air. The Nyquist plots were measured on an IM6 electrochemical workstation (Zahner Zennium, Germany) in the dark with a bias near the respective V_{OC} of individual cells. For PL mapping, a JMAT-S confocal laser scanning microscope (SouthPort Co., Ltd, Taiwan) was used, the excitation wavelength was 445 nm, and the confocal pinhole was set to 50 μm size with an a×10 objective. The measurements of PL spectra were conducted on an FLS 980

(Edinburgh Instrument, UK). Time-resolved PL measurements were acquired on a Lifespec II (Edinburgh Instrument, UK). The transient PL spectra were collected by monitoring the signal at 780 nm excited with a 477 nm laser (2 MHz). The TPV and TPC spectra were obtained from TPVC-1G (SouthPort Co., Ltd, Taiwan). XPS was recorded on an ESCALAB 250Xi instrument (Thermo Fisher, USA). Ultraviolet Photoelectron Spectroscopy (UPS) was performed by PHI 5000 VersaProbe III with He I source (21.22 eV) under an applied negative bias of 9.0 V.

SEM and EDS images were acquired on a Hitachi SU8010 SEM, and the distribution of the perovskite grain size was analyzed using Nano Measurer 1.2 software. The contact angles were measured by a KRÜSS DSA100 surface analysis system. AFM images were captured using a MultiMode 8 microscope (Bruker, Santa Barbara, CA) with peak force quantitative nanomechanical mode in air. Fourier transform infrared (FTIR) spectra were measured with a Bruker VERTEX 70 V. All the performances of the devices were measured immediately after fabrication.

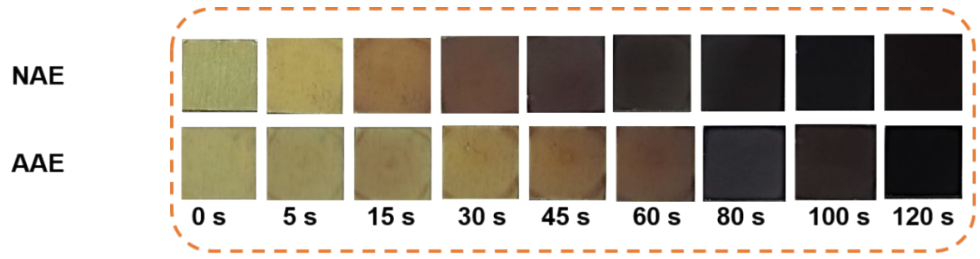

Fig. S1. Photographs of NAE- and AAE-treated perovskite films were annealed at 70 °C at different times.

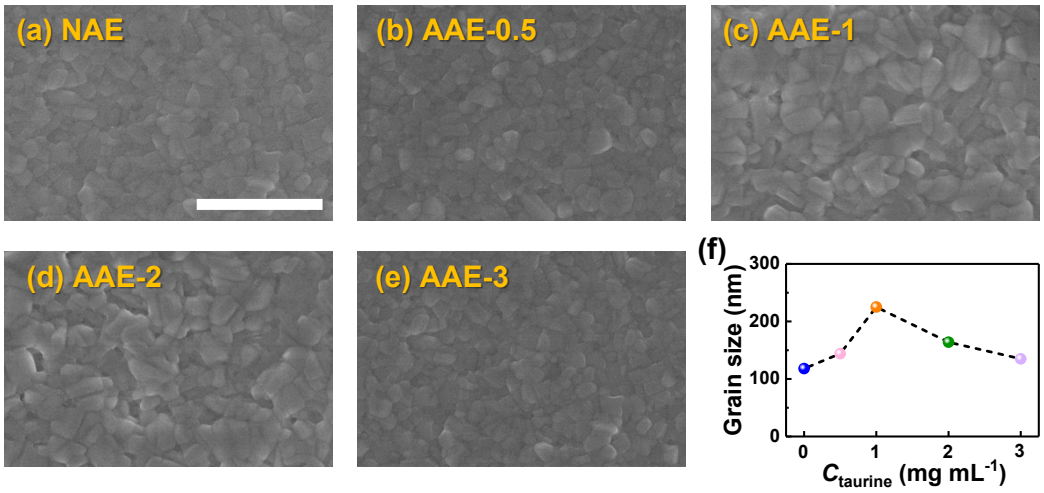

Fig. S2. Top-view SEM images of perovskite films treated with (a) NAE, (b) AAE-0.5, (c) AAE-1, (d) AAE-2 and (e) AAE-3.

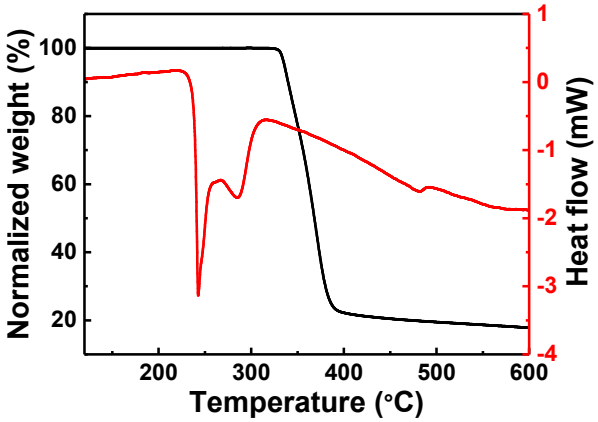

Fig. S3. Thermogravimetric analysis (TGA) of taurine measured under N_2 protection with a heating rate of 10 °C/min.

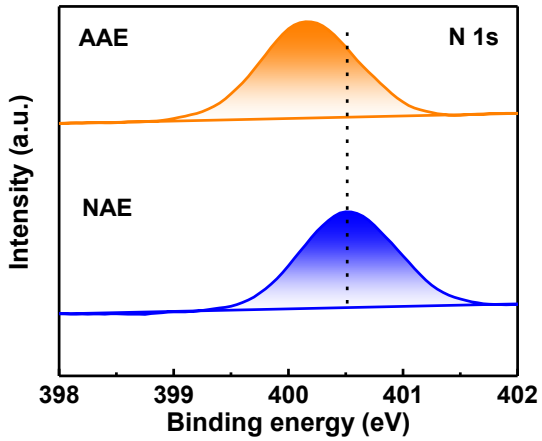

Fig. S4. XPS spectral N 1s of the perovskite films treated with NAE and AAE.

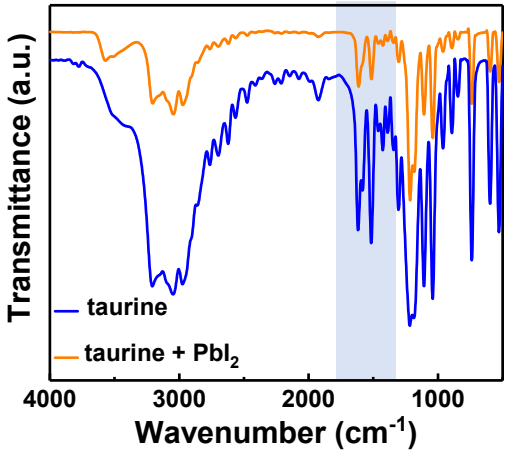

Fig. S5. The Fourier transform infrared (FTIR) spectra of taurine and a mixture of PbI_2 and taurine.

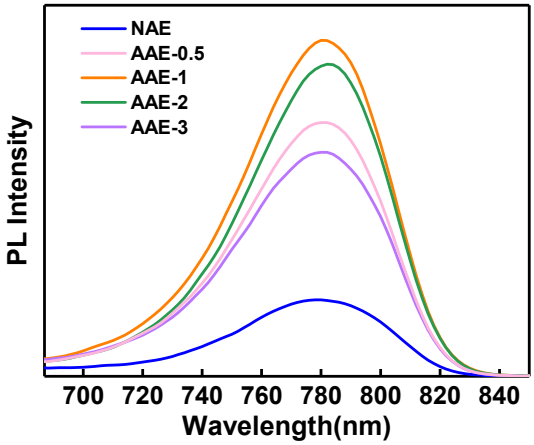

Fig. S6. Steady-state photoluminescence (PL) spectra of the AAE-treated perovskite films with different taurine concentrations.

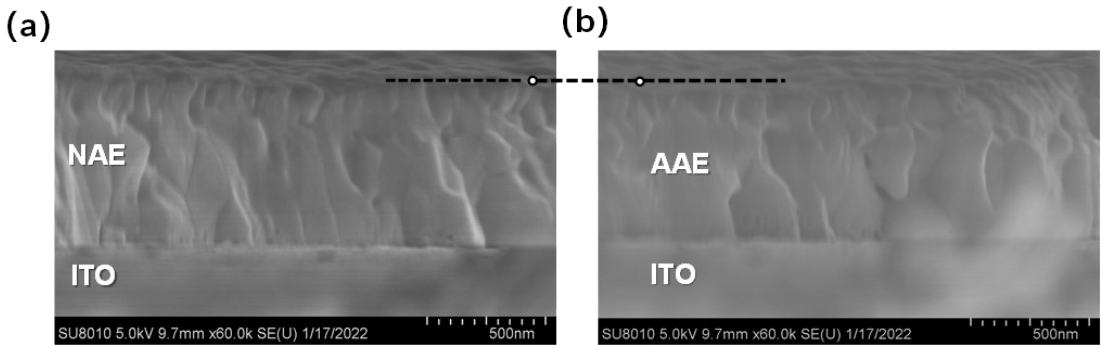

Fig. S7. Cross-sectional SEM images of perovskite films (a) NAE and (b) AAE.

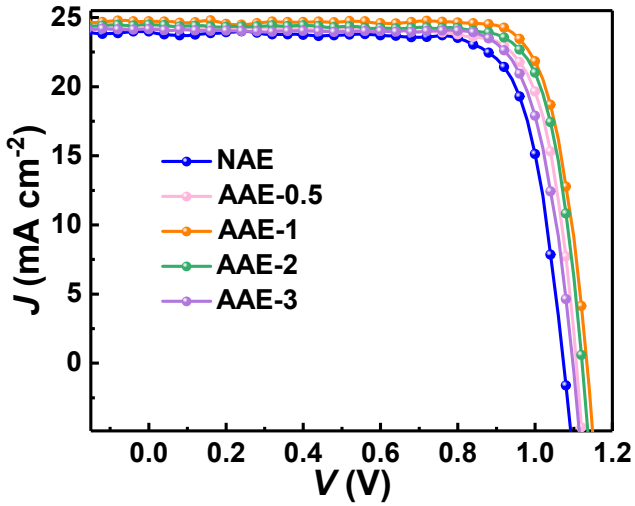

Fig. S8. *J-V* curves of the AAE-treated Pero-SCs with different $C_{taurine}$s.

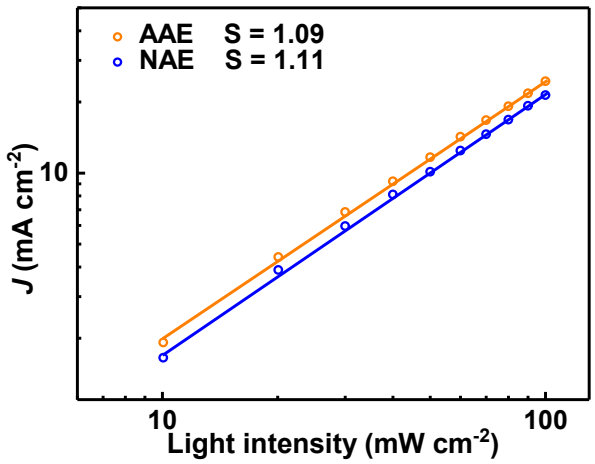

Fig. S9. J_{sc} versus light intensity of Pero-SCs treated with NAE and AAE.

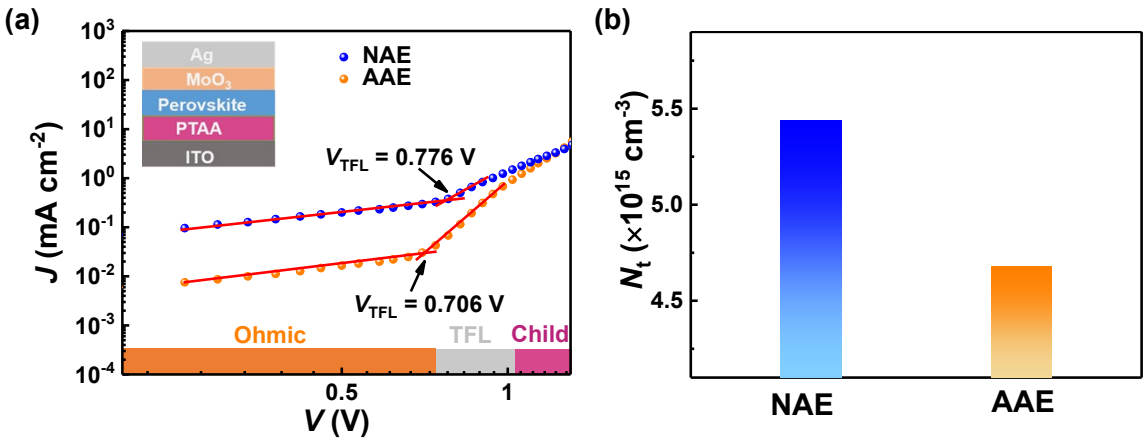

Fig. S10. Dark *J*−*V* curves of hole-only perovskite films treated with NAE and AAE for SCLC analysis.

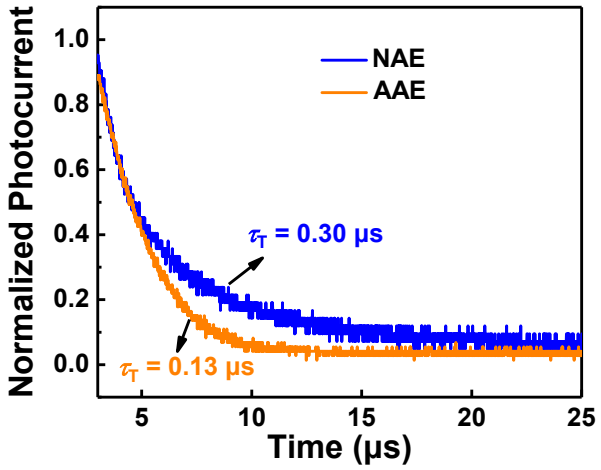

Fig. S11. Normalized transient photocurrent (TPC) decay of Pero-SCs.

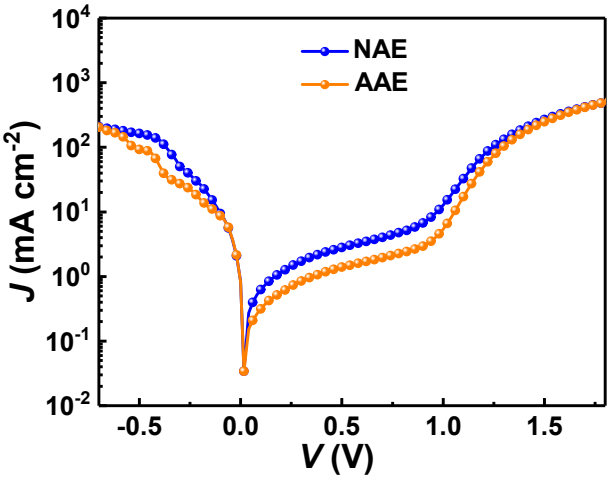

Fig. S12. *J*-*V* curves of Pero-SCs were measured in the dark.

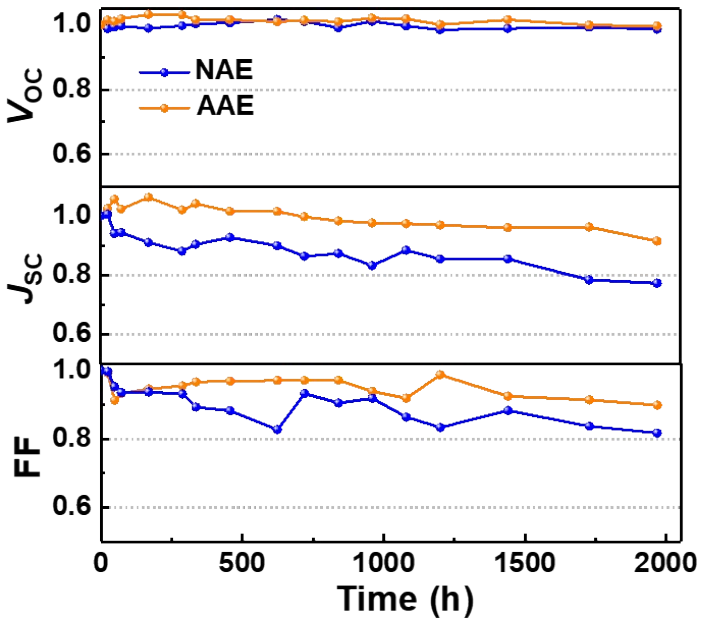

Fig. S13. Thermal stability test of normalized V_{OC}, J_{SC}, and FF of the devices treated with NAE and AAE under heating in a N_2 environment (70 °C).

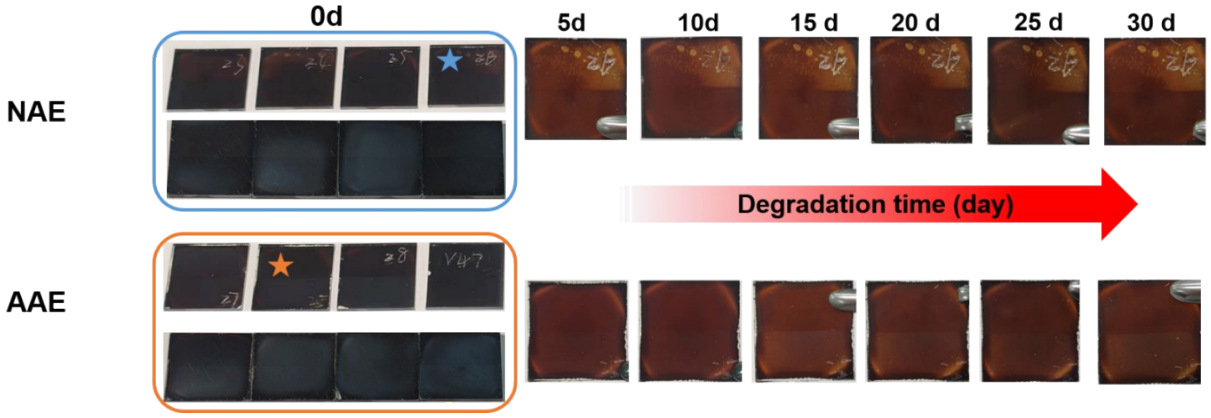

Fig. S14. Photographs of perovskite degradation of the perovskite films treated with NAE and AAE in ambient air (RH = 40 ± 10%).

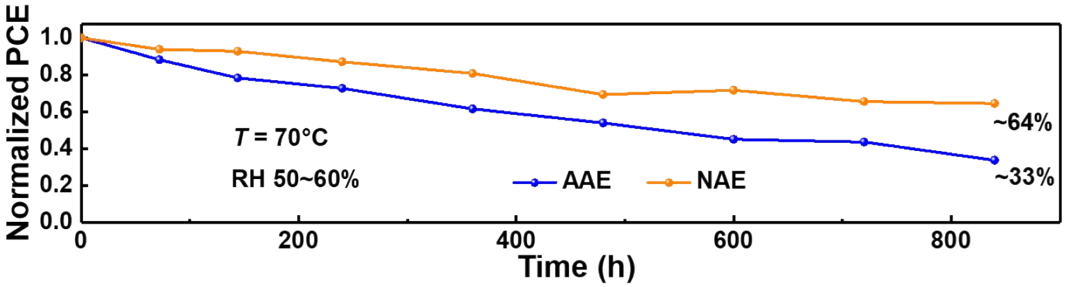

Fig. S15.The damp heat stability ($T \approx 70$ °C, RH 50~60%) of the Pero-SCs treated with NAE and AAE.

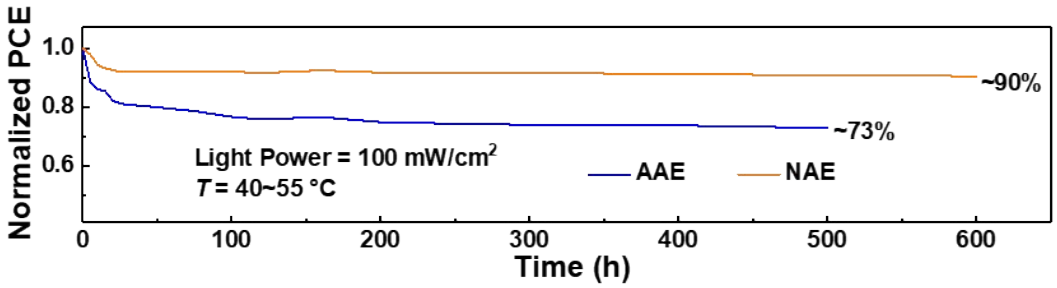

Fig.S16. The light soaking stability of Pero-SCs treated with NAE and AAE under continuous AM 1.5G (100 mW cm^{-2}) at MPP in a N_2 environment.

Table S1. Photovoltaic parameters of Pero-SCs depend on different $C_{taurine}$s.

$C_{taurine}$ (mg/mL)	V_{OC} (V)	J_{SC} (mA cm^{-2})	FF (%)	PCE (%)
0	1.07	23.94	77.0	19.73
0.5	1.11	24.31	78.4	20.97
1	1.13	24.72	80.2	22.54
2	1.12	24.48	79.3	21.67
3	1.10	24.14	78.5	20.61

Table S2. Photovoltaic parameters of the Pero-SCs treated with NAE and AAE under reverse scan (RS) and forward scan (FS) directions.

		V_{OC} (V)	J_{SC} (mA cm^{-2})	FF (%)	PCE (%)	Hysteresis index
NAE	FS	1.08	23.52	77.0	19.50	0.10
	RS	1.06	22.01	75.3	17.53	
AAE	FS	1.12	24.71	78.7	21.57	0.04
	RS	1.11	24.02	77.9	20.64	

Table S3. Fitted parameters from ACIS of the Pero-SCs.

	R_s (Ω)	R_{tr} (Ω)	C_{tr} (F)	R_{rec} (Ω)	C_{rec} (F)
NAE	30.5	178.1	4.5×10^{-9}	55.7	1.4×10^{-8}
AAE	29.8	33.2	1.3×10^{-8}	67.6	6.2×10^{-9}